

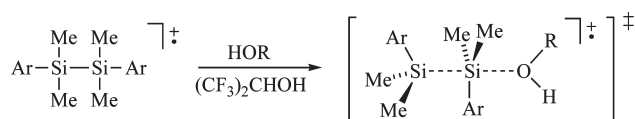
## Generation and Characterization of 1,2-Diaryl-1,1,2,2-tetramethyldisilane Cation Radicals

Gonzalo Guirado,<sup>†</sup> Olesya Haze, and Joseph P. Dinnocenzo\*

Department of Chemistry and the Center for Photoinduced Charge Transfer, University of Rochester, Rochester, New York 14627-0216. <sup>†</sup>Present address: Universitat Autònoma de Barcelona, Departament de Química (Química-Física), Edifi C, 08193-Bellaterra (Barcelona), Spain (e-mail: gonzalo.guirado@uab.es).

jpd@chem.rochester.edu

Received February 25, 2010



Nanosecond laser flash photolysis methods were used to generate and spectrally characterize the cation radicals of 1,2-diaryl-1,1,2,2-tetramethyldisilanes (Ar = *p*-X-Ph, X = H, CH<sub>3</sub>, OCH<sub>3</sub>) in hexafluoroisopropanol (HFIP) at room temperature. The disilane cation radicals rapidly reacted with methanol, with bimolecular rate constants ranging from 0.63 to 2.1 × 10<sup>8</sup> M<sup>-1</sup> s<sup>-1</sup>. The cation radicals were found to react with *tert*-butanol 4–5 times more slowly than methanol, consistent with a small steric effect for nucleophile-assisted fragmentation of the Si–Si bond. The standard potentials for oxidation of the disilanes in HFIP were determined by two different methods: first, by measuring equilibrium constants for electron exchange between the disilanes and the cation radical of hexaethylbenzene and, second, by combining electrochemical data from cyclic voltammetry with the lifetimes of the disilane cation radicals measured by laser flash photolysis in the same media. Agreement between the two methods was excellent (≤3 mV). The oxidation of 1,2-di-*p*-methoxyphenyl-1,1,2,2-tetramethyldisilane by slow scan cyclic voltammetry in acetonitrile was not found to be reversible, in contrast to prior literature reports. Possible explanations for the prior results are proposed.

### Introduction

One-electron oxidation of disilanes under a variety of conditions leads to fragmentation of the Si–Si bond.<sup>1</sup> The fragmentation mechanism of the disilane cation radical intermediates is uncertain for the vast majority of these reactions—both unimolecular and nucleophile-assisted pathways have been proposed. Most of the mechanistic evidence gathered to date that supports a nucleophile-assisted mechanism has been indirect.

For example, electron impact ionizations of disilanes containing a tethered alcohol do not show molecular ion peaks, consistent with rapid intramolecular nucleophilic substitution on the parent ion.<sup>1f</sup> In addition, photooxidation of several unsymmetrically substituted disilanes preferentially gave products that could be rationalized from reaction of nucleophiles at the less sterically hindered silicon atom.<sup>1g</sup> Finally, the unusually low oxidation potential found for 1,2-bis(2-(2-pyridyl)phenyl)-1,1,2,2-tetramethyldisilane can be explained by intramolecular coordination during one-electron oxidation.<sup>1j</sup> Only recently has kinetic evidence been reported that the cation radical of the highly sterically hindered 1,1,2,2-tetra-*tert*-butyl-1,2-diphenyldisilane reacts with methanol in a bimolecular reaction.<sup>1i</sup>

It has been generally assumed that disilane cation radicals are highly reactive intermediates with short lifetimes under normal experimental conditions.<sup>2</sup> It is surprising, therefore,

(1) (a) Watanabe, H.; Kato, M.; Tabei, E.; Kuwabara, H.; Hirai, N.; Sato, T.; Nagai, Y. *J. Chem. Soc., Chem. Commun.* **1986**, 1662. (b) Mizuno, K.; Nakanishi, K.; Chosa, J.; Nguyen, T.; Otsuji, Y. *Tetrahedron Lett.* **1989**, 30, 3689. (c) Fukuzumi, S.; Kitano, T.; Mochida, K. *Chem. Lett.* **1989**, 2177. (d) Fukuzumi, S.; Kitano, T.; Mochida, K. *J. Chem. Soc., Chem. Commun.* **1990**, 1236. (e) Nakadaira, Y.; Sekiguchi, A.; Funada, Y.; Sakurai, H. *Chem. Lett.* **1991**, 327. (f) Nakadaira, Y.; Otani, S.; Kyushin, S.; Ohashi, M.; Sakurai, H.; Funada, Y.; Sakamoto, K.; Sekiguchi, A. *Chem. Lett.* **1991**, 601. (g) Mizuno, K.; Nakanishi, K.; Chosa, J.; Otsuji, Y. *J. Organomet. Chem.* **1994**, 473, 35. (h) Kako, M.; Nakadaira, Y. *Bull. Chem. Soc. Jpn.* **2000**, 73, 2403. (i) Al-Kaysi, R. O.; Goodman, J. L. *J. Am. Chem. Soc.* **2005**, 127, 1620. (j) Nokami, T.; Soma, R.; Yamamoto, Y.; Kamei, T.; Itami, K.; Yoshida, J. *Beilstein J. Org. Chem.* **2007**, 3.

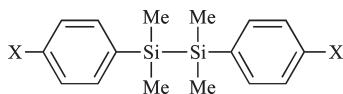
(2) See, for example: Kako, M.; Hatakenaka, K.; Kakuma, S.; Ninomiya, M.; Nakadaira, Y.; Yasui, M.; Iwasaki, F.; Wakasa, M.; Hayashi, H. *Tetrahedron Lett.* **1999**, 40, 1133.

that 1,2-di-*p*-anisyl-1,1,2,2-tetramethyldisilane (**1**) and several related disilanes have been reported to be reversibly oxidized electrochemically by slow scan (0.1–0.2 V/s) cyclic voltammetry in CH<sub>3</sub>CN at room temperature.<sup>3</sup>

We describe herein the generation of **1**<sup>•+</sup> by nanosecond laser flash photolysis and demonstrate that it has an extremely short lifetime (< 100 ns) in CH<sub>3</sub>CN. Consistent with this observation, electrochemical oxidation of **1** by cyclic voltammetry is *not* reversible in CH<sub>3</sub>CN. Generation of **1**<sup>•+</sup> is possible in the nonnucleophilic solvent (CF<sub>3</sub>)<sub>2</sub>CHOH, although only as a highly reactive, transient intermediate. We provide direct kinetic evidence that **1**<sup>•+</sup> and related disilane cation radicals undergo rapid Si–Si bond fragmentation by a nucleophile-assisted mechanism. In addition, we describe several methods to determine reliable oxidation potentials for **1** and several structurally related disilanes.

## Results

**Generation and Reaction of Disilane Cation Radicals with Nucleophiles.** Our first experimental goal was to determine if disilane cation radicals could be generated and spectroscopically characterized in solution at room temperature. Disilanes **1**–**3** were chosen for initial study. One-electron oxidation of the disilanes was accomplished by nanosecond pulsed laser excitation (7 ns, 343 nm) of solutions containing ~1 mM *N*-methylquinolinium hexafluorophosphate (NMQ<sup>+</sup>) as a photooxidant and toluene as a codonor. Although this system for generating radical cations has been described in detail elsewhere,<sup>4</sup> we outline here its essential features for clarity. Pulsed laser excitation of NMQ<sup>+</sup> produces its singlet-excited state (<sup>1</sup>NMQ<sup>•+</sup>), which is rapidly intercepted by toluene, which is present in high concentration (1 M), to efficiently produce toluene<sup>•+</sup> and the *N*-methylquinolinyl radical (NMQ<sup>•</sup>) via photoinduced electron transfer. Reaction of the disilanes, which are present in lower concentration (20–50 mM) than toluene, with toluene<sup>•+</sup> by electron transfer is expected to be highly exothermic and, therefore, should rapidly generate the disilane cation radicals. In cases where the absorption of NMQ<sup>•</sup> ( $\lambda_{\max} \approx 540$  nm) is problematic, it can be rapidly scavenged (< 100 ns) in dioxygen-saturated solution leading to O<sub>2</sub><sup>•-</sup>, which does not have interfering absorptions in the visible region where cation radicals typically absorb.



- 1:** X = OMe  
**2:** X = Me  
**3:** X = H

In nanosecond, pulsed laser experiments with NMQ<sup>+</sup>, toluene, and disilanes **1**–**3** in acetonitrile, no transient absorptions between 350 and 800 nm (except for NMQ<sup>•</sup>) with lifetimes greater than ~100 ns were observed. In contrast, when the experiments were conducted in the less nucleophilic solvent hexafluoroisopropanol (HFIP),<sup>5</sup> transients were

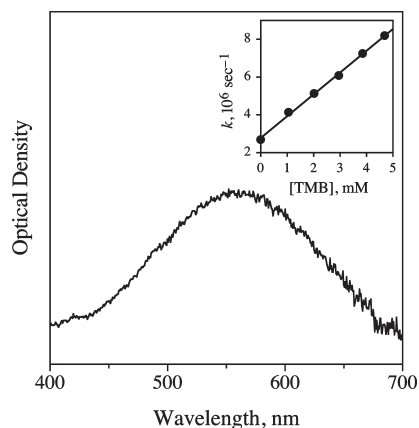


**FIGURE 1.** Transient spectrum produced from pulsed laser photolysis of a O<sub>2</sub>-saturated HFIP solution containing NMQ<sup>+</sup>, toluene, and **3**. Inset: Plot of the pseudo-first-order decay rate constant at 560 nm vs [TMB].

observed with all three disilanes. For example, in O<sub>2</sub>-saturated HFIP, photolysis of NMQ<sup>+</sup>/toluene solutions containing **3** (~50 mM) gave a new transient with  $\lambda_{\max} \approx 560$  nm (Figure 1). The lifetime of this transient was found to increase from ~150 ns when no special precautions were used to remove adventitious water to > 600 ns when solutions were dried over molecular sieves. The transient species was found to react with the good electron donors such as 1,2,4,5-tetramethoxybenzene (TMB,  $E_{\text{ox}} = 0.88$  V vs SCE).<sup>6</sup> A plot of the pseudo-first-order rate constant for decay at 560 nm vs [TMB] was linear (see Figure 1 inset) and the slope of the plot gave a second-order rate constant of  $1.3 \times 10^9 \text{ M}^{-1} \text{ s}^{-1}$ , which is near the diffusion limit in HFIP.<sup>7</sup> Concomitant with disappearance of the 560 nm transient, a relatively long-lived transient appeared with  $\lambda_{\max} \approx 460$  nm, which was identical to independently generated TMB<sup>•+</sup>. These data are consistent with the assignment of the 560 nm transient species to **3**<sup>•+</sup>. This assignment is further supported by the spectral similarity to **3**<sup>•+</sup> previously generated in a Freon matrix at 77K ( $\lambda_{\max} \approx 580$  nm).<sup>8</sup> Transient species were also observed with disilanes **1** ( $\lambda_{\max} \approx 800$ )<sup>9</sup> and **2** ( $\lambda_{\max} \approx 650$ ). These transients were also found to react with TMB to generate TMB<sup>•+</sup>, consistent with their assignment to **1**<sup>•+</sup> and **2**<sup>•+</sup>. The lifetimes of **1**<sup>•+</sup> and **2**<sup>•+</sup> were ~1200 and ~900 ns, respectively, in dry HFIP. Importantly, attempted generation of **1**<sup>•+</sup>—the longest lived disilane cation radical—in acetonitrile gave a weak transient that completely decayed within 100 ns. We will return to the significance of this observation when discussing the electrochemical oxidation of the disilanes.

(5) For use of HFIP as a non-nucleophilic solvent, see: (a) Ebersson, L.; Hartshorn, M. P.; Persson, O. *J. Chem. Soc., Perkin Trans. 2* **1995**, 1735. (b) Kirmse, W.; Krzossa, B.; Steenken, S. *Tetradedron Lett.* **1996**, 1197. (c) Pienta, N. J.; Kessler, R. *J. Am. Chem. Soc.* **1993**, *115*, 8330. (d) Cozens, F.; Li, J.; McClelland, R. A.; Steenken, S. *Angew. Chem., Int. Ed. Engl.* **1992**, *31*, 743. (e) Kirmse, W.; Kilian, J.; Steenken, S. *J. Am. Chem. Soc.* **1990**, *112*, 6399.

(6) de Lijser, H. J. P.; Snelgrove, D. W.; Dinnocenzo, J. P. *J. Am. Chem. Soc.* **2001**, *123*, 9698.

(7) The diffusion rate constant ( $k_d$ ) in HFIP can be estimated from the Smoluchowski equation ( $k_d \approx 8RT/(3000\eta) \text{ M}^{-1} \text{ s}^{-1}$ ) to be  $\sim 3 \times 10^9 \text{ M}^{-1} \text{ s}^{-1}$  at 20 °C, with  $\eta = 1.94$  cP: Murto, J.; Kivinen, A.; Lindell, E. *Suom. Kemistil. B* **1970**, *43*, 28.

(8) Kumagai, J.; Yoshida, H.; Ichikawa, T. *J. Phys. Chem.* **1995**, *99*, 7965.

(9) The  $\lambda_{\max}$  of **1**<sup>•+</sup> cannot be as well determined as that of **2**<sup>•+</sup> and **3**<sup>•+</sup> due to the limited amount of analyzing light beyond 800 nm in our nanosecond laser apparatus.

(3) (a) Zhuikov, V. V. *Russ. J. Gen. Chem.* **1997**, *67*, 975. (b) Zhuikov, V. V. *Russ. J. Gen. Chem.* **2000**, *70*, 879. (c) Zhuikov, V. V. *Russ. J. Electrochem.* **2000**, *36*, 117.

(4) Dockery, K. P.; Dinnocenzo, J. P.; Farid, S.; Goodman, J. L.; Gould, I. R.; Todd, W. P. *J. Am. Chem. Soc.* **1997**, *119*, 1876.

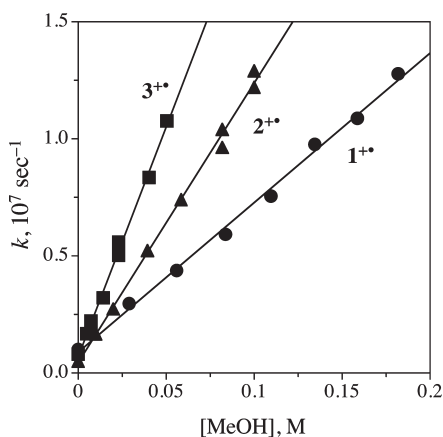


**FIGURE 2.** Plot of the pseudo-first-order rate constants for decay of  $1^{2+}$ – $3^{2+}$  in HFIP as a function of the concentration of added methanol.

Disilane cation radicals  $1^{2+}$ – $3^{2+}$  were found to rapidly react with deliberately added nucleophiles, such as alcohols. Shown in Figure 2 is a plot of the pseudo-first-order rate constants for decay of the transients vs [HOME]. The corresponding second-order rate constants are given in Table 1. Kinetic plots with added HOBu<sup>t</sup> were also linear; the second-order rate constants from these plots are listed in Table 1. The rate constant ratio  $k_{\text{HOME}}/k_{\text{HOBu}^t}$  was found to be small and nearly independent of the disilane cation radical structure (see Table 1).

**Oxidation Potentials of 1–3 by Redox Equilibrium.** As shown in Table 1, the rate constants for reaction of  $1^{2+}$ – $3^{2+}$  with HOME or HOBu<sup>t</sup> vary by less than a factor of 4. Interestingly, this is substantially smaller than the rate constant range of > 65 observed for the reaction of HOME with benzyltrimethylsilane cation radical vs the *p*-methoxybenzyl derivative.<sup>4</sup> The large difference in reactivity of the benzylsilane cation radicals has been correlated with their relative oxidation potentials, which differ by nearly ~0.5 V.<sup>10</sup> It was, therefore, of interest to determine the oxidation potentials of 1–3. Given the short lifetimes of  $1^{2+}$ – $3^{2+}$  described above, the one-electron oxidations of 1–3 with conventional electrochemical methods are not expected to be reversible. Indeed, as described in the next section, they are not.

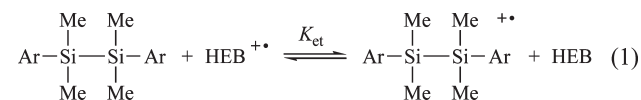
The oxidation potentials of 1–3 in HFIP were determined by two different methods. The first was by redox equilibration. This method, which is described in detail elsewhere,<sup>11,12</sup> involves measuring the equilibrium constant for electron transfer between a compound of unknown oxidation potential and the cation radical of a compound whose reduction potential is known. It turned out that hexaethylbenzene (HEB) served as a suitable reference compound for disilanes 1–3. The oxidation of HEB is fully reversible in HFIP ( $E_{\text{ox}} = 1.114(3)$ <sup>13</sup> V vs SCE). The redox equilibrium between

**TABLE 1.** Substituent Effects on the Second-Order Rate Constants for the Reaction of Disilane Cation Radicals  $1^{2+}$ – $3^{2+}$  with Methanol ( $k_{\text{HOME}}$ ) and *tert*-Butanol ( $k_{\text{HOBu}^t}$ ) in HFIP at 20 °C

disilane <sup>2+</sup>	rate constants, <sup>a</sup> M <sup>-1</sup> s <sup>-1</sup>		
	$k_{\text{HOME}}$	$k_{\text{HOBu}^t}$	$k_{\text{HOME}}/k_{\text{HOBu}^t}$
$1^{2+}$	$6.3(2) \times 10^7$	$1.3(2) \times 10^7$	4.8
$2^{2+}$	$1.3(1) \times 10^8$	$2.9(2) \times 10^7$	4.5
$3^{2+}$	$2.1(2) \times 10^8$	$4.9(2) \times 10^7$	4.3

<sup>a</sup>Rate constants are an average of at least three independent determinations; standard deviation in the last significant digit is given in parentheses.

the disilanes and HEB was set up by using experimental conditions similar to those used to generate  $1^{2+}$ – $3^{2+}$ . Pulsed laser excitation of a O<sub>2</sub>-saturated HFIP solution containing NMQ<sup>+</sup> and toluene (1 M) generated the toluene cation radical subsequently oxidized the disilane and HEB, which were present in solution at lower concentration (~1–20 mM). The spectra for the disilane cation radical and HEB<sup>2+</sup> were monitored until an equilibrium was reached for the electron transfer reaction (eq 1). The electron transfer equilibrium constants ( $K_{\text{et}}$ ) were calculated from  $[\text{disilane}^{2+}][\text{HEB}]/[\text{disilane}][\text{HEB}^{2+}]$ . At low pulse energies, where the concentrations of the radical cations ( $\leq 10^{-5}$  M) are very small compared to those of the neutral species, [disilane] and [HEB] are indistinguishable from their initial concentrations. The difference in oxidation potential between the disilane and HEB ( $\Delta E_{\text{ox}}$ ) was calculated from the Nernst equation (eq 2).



$$\Delta E_{\text{ox}} = E_{\text{ox}}(\text{disilane}) - E_{\text{ox}}(\text{HEB}) = -(RT/F) \ln K_{\text{et}} \quad (2)$$

Shown in Figure 3 are typical redox equilibrium spectra for HEB and 3. Spectra of HEB<sup>2+</sup> and 3<sup>2+</sup> are given by traces a and b, respectively. Equilibrium mixtures of the two cation radicals at three different concentrations of HEB and 3 are also shown. An isosbestic point is observed at ~530 nm, as expected for the simple, electron transfer equilibrium in eq 1. As described before,<sup>12</sup> the equilibrium spectra can be fit with linear combinations of the pure cation radical spectra. Fitting of the equilibrium spectra in Figure 3 gave an average value for  $K_{\text{et}}$  of 3.0(4). The average value of  $K_{\text{et}}$  from several independent experiments was 2.8(4). This value of  $K_{\text{et}}$  corresponds to  $E_{\text{ox}}(3) - E_{\text{ox}}(\text{HEB}) = -0.026(4)$  V. The error in  $\Delta E_{\text{ox}}$  is small (4 mV), but typical of the high precision that can be obtained by the redox equilibrium method. Combining  $\Delta E_{\text{ox}}$  with  $E_{\text{ox}}(\text{HEB})$  gives  $E_{\text{ox}}^{\text{c}}(3) = 1.088(5)$  V vs SCE in HFIP. Analogous redox equilibrium experiments were carried out with 1 and 2, which form long-lived disilane cation radicals, with equally good results. The oxidation potentials from redox equilibrium measurements with 1/HEB and 2/HEB are given in Table 2.

**Oxidation Potentials of Disilanes 1–3 from Cyclic Voltammetry in HFIP.** Given the short lifetimes of  $1^{2+}$ – $3^{2+}$  in HFIP, the oxidations of 1–3 are not expected to be reversible by conventional cyclic voltammetry. Indeed, they are not.

(10) Dinnocenzo, J. P.; Farid, S.; Goodman, J. L.; Gould, I. R.; Todd, W. P.; Mattes, S. L. *J. Am. Chem. Soc.* **1989**, *111*, 8973.

(11) For reviews, see: (a) Steenken, S. *Landolt-Börnstein* **1985**, *13e*, 147. (b) Wardman, P. *J. Phys. Chem. Ref. Data* **1989**, *18*, 1637. (c) Stanbury, D. M. In *General Aspects of the Chemistry of Radicals*; Alfassi, Z. B., Ed.; Wiley: New York, 1999; Chapter 11.

(12) (a) Guirado, G.; Fleming, C. N.; Lingenfelter, T. G.; Williams, M. L.; Zuillhof, H.; Dinnocenzo, J. P. *J. Am. Chem. Soc.* **2004**, *126*, 14086. (b) Merkel, P. B.; Luo, P.; Dinnocenzo, J. P.; Farid, S. *J. Org. Chem.* **2009**, *74*, 5163.

(13) Standard deviation of the last significant digit is given in parentheses.

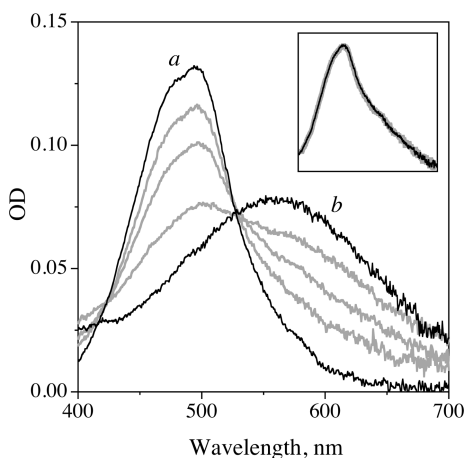


**FIGURE 3.** Spectra of hexaethylbenzene cation radical (a),  $3^{+\bullet}$  (b), and the equilibrium, electron transfer spectra (gray lines) in HFIP at 20 °C. Inset: One of the equilibrium spectra (gray line) and the best least-squares fit to it (thin black line).

**TABLE 2.** Differences in Oxidation Potentials for Disilanes 1–3 and HEB ( $\Delta E_{\text{ox}}$ ) Determined from Redox Equilibrium Measurements in HFIP at 20 °C, Oxidation Potentials for 1–3 ( $E_{\text{ox}}^{\text{eq}}$ ) Based on  $\Delta E_{\text{ox}}$ , and Formal Oxidation Potentials ( $E^{\circ'}$ ) from Cyclic Voltammetry–Laser Flash Photolysis

disilane	$(\Delta E_{\text{ox}})^a$	$(E_{\text{ox}}^{\text{eq}})^b$	$(E^{\circ'})^c$
1	−0.045(3)	1.069(4)	1.067(4)
2	−0.032(4)	1.082(5)	1.083(5)
3	−0.026(4)	1.088(5)	1.091(3)

<sup>a</sup>Average  $E_{\text{ox}}(\text{disilane}) - E_{\text{ox}}(\text{HEB})$ , V; standard deviation in the last significant digit is given in parentheses. <sup>b</sup> $E_{\text{ox}}^{\text{eq}} = (\text{HEB}) + \Delta E_{\text{ox}}$ ; V vs SCE. <sup>c</sup>Formal oxidation potential from cyclic voltammetry–laser flash photolysis in HFIP at 20 °C, V vs SCE (see text).

In principle, it is nonetheless possible to determine the disilane oxidation potentials if the lifetimes of  $1^{+\bullet}$ – $3^{+\bullet}$  are known under the reaction conditions by using well-known electrochemical relationships between the peak potential and the scan rate. Determination of the cation radical lifetimes by laser flash photolysis on electrochemical solutions provided a rare opportunity<sup>14</sup> to obtain independent measurements of the disilane oxidation potentials. To accomplish this objective, it was first necessary to better characterize the electrooxidation process.

The electrochemical oxidations of 1–3 by cyclic voltammetry using a glassy carbon electrode as a working electrode were not reversible in HFIP at scan rates varying from 0.1 to 50  $\text{V s}^{-1}$ . The anodic peak potential currents ( $i_{\text{pa}}$ ) increased linearly with the concentrations of the disilanes ( $C = 1$ – $15$  mM) and with the square root of the scan rate ( $\nu^{1/2}$ ). The ratio of  $i_{\text{pa}}/C\nu^{1/2}$  remained constant over the entire scan rate range and a comparison of the ratio to that measured for ferrocene under identical conditions provided the number of electrons transferred (1.8–1.9). At a scan rate of 0.1 V/s, the peak widths ( $E_{\text{pa}} - E_{\text{pa}/2}$ ) for the oxidation waves were  $56 \pm 2$  mV and were independent of disilane concentration. Plots of the anodic peak potentials ( $E_{\text{pa}}$ ) vs  $\log(\nu)$  were linear and had slopes of  $32 \pm 2$  V/ $\log(\nu)$  (Figure 4, unfilled symbols). These data are consistent with fast heterogeneous electron transfer at the electrode followed by a rapid first-order (or

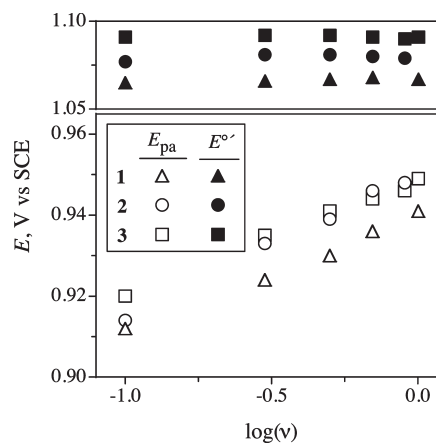


**FIGURE 4.** Anodic peak potentials ( $E_{\text{pa}}$ ) for disilanes 1–3 as a function of the logarithm of the scan rate ( $\nu$ ,  $\text{V s}^{-1}$ ) in HFIP. Formal oxidation potentials ( $E^{\circ'}$ ) calculated from eq 3 for 1–3 as a function of the logarithm of the scan rate.

pseudo-first-order) reaction of the disilane cation radicals and, finally, a second electron transfer from the products of the chemical reaction, i.e., an ECE mechanism. Taking into account the results from the above laser flash photolysis experiments, the oxidations of 1–3 can be explained by one-electron oxidation of the disilanes followed by rapid nucleophilic substitution by the solvent. The leaving groups from the substitution—the aryldimethylsilyl radicals—presumably undergo rapid oxidation at the electrode, thus accounting for the two-electron wave.<sup>15</sup>

The preliminary electrochemical experiments demonstrate that 1–3 undergo rapid oxidation at the electrode surface. On the basis of this observation, the anodic potentials ( $E_{\text{pa}}$ ) for the electrochemical oxidations are expected to follow eq 3,<sup>16</sup> where  $E^{\circ'}$  is the formal oxidation potential,  $k$  is the rate constant for the chemical reaction coupled to the electron transfer,  $\nu$  is the scan rate, and  $n$  is the number of electrons transferred in the initial oxidation ( $R$ ,  $T$ , and  $F$  have their usual meaning). The rate constants for decay of  $1^{+\bullet}$ – $3^{+\bullet}$  were measured by laser flash photolysis from the same solutions (including electrolyte, 0.1 M  $n\text{-Bu}_4\text{N}^+\text{BF}_4^-$ ) previously used to determine the variation of  $E_{\text{pa}}$  as a function of  $\log(\nu)$ . The values of  $E^{\circ'}$  were calculated at each scan rate from the  $E_{\text{pa}}$  values and the cation radical decay rate constant ( $k$ ) by using eq 3. Gratifyingly, the calculated  $E^{\circ'}$  values for all three disilanes were found to be independent of scan rate (Figure 4, filled symbols). As shown in Table 2, the formal potentials derived from the combined electrochemistry–laser flash photolysis experiment are in excellent agreement with those determined by the redox equilibrium method.

$$E_{\text{pa}} = E^{\circ'} + 0.780 \frac{RT}{nF} - \frac{RT}{2nF} \ln \left[ \frac{k RT}{\nu nF} \right] \quad (3)$$

**Cyclic Voltammetry of 1 in  $\text{CH}_3\text{CN}$ .** On the basis of the extremely short lifetime of  $1^{+\bullet}$  in  $\text{CH}_3\text{CN}$  estimated from

(14) For an elegant use of this approach, see: Gould, I. R.; Wosinska, Z. M.; Farid, S. *Photochem. Photobiol.* **2006**, *82*, 104.

(15) The electrochemical experiment was performed under an argon atmosphere, otherwise the silyl radicals might have partially reacted with dioxygen present in solution (cf.: Mizuno, K.; Tamai, T.; Hashida, I.; Otsuji, Y. *J. Org. Chem.* **1995**, *60*, 2935).

(16) Nicholson, R. S.; Shain, I. *Anal. Chem.* **1964**, *36*, 706.

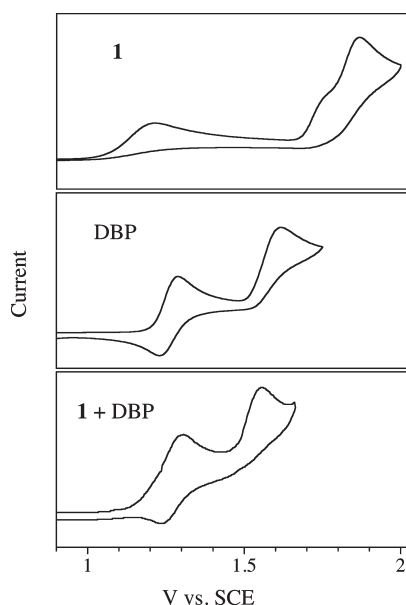


**FIGURE 5.** Cyclic voltammograms (single scan) of disilane **1** (5.0 mM, top), 4,4'-dimethoxybiphenyl (DBP, 12 mM, middle), and a solution containing 2.5 mM **1** and 5.8 mM DBP (bottom) in acetonitrile containing 0.1 M tetra-*n*-butylammonium tetrafluoroborate recorded with a scan rate of 0.50 V s<sup>-1</sup>.

laser flash photolysis ( $\tau < 100$  ns), it is not surprising that the oxidation of **1** by cyclic voltammetry in CH<sub>3</sub>CN was *not* found to be reversible. This result is in disagreement, however, with earlier reports<sup>3</sup> that **1** and several related disilanes are reversibly oxidized in CH<sub>3</sub>CN at room temperature at low scan rates. These reports claim that **1** exhibits a reversible CV wave at  $\sim 1.3$  V vs SCE and a second, irreversible wave at  $\sim 1.7$  V. We find that oxidation of **1** in CH<sub>3</sub>CN shows irreversible oxidation waves at  $\sim 1.2$  and  $\sim 1.9$  V vs SCE (Figure 5, top panel). The reversible wave previously reported at  $\sim 1.3$  V is consistent with that observed for 4,4'-dimethoxybiphenyl (DBP),<sup>17</sup> a plausible contaminant from the preparation of **1**.<sup>18</sup> Indeed, when we deliberately add DBP to a solution containing **1** (Figure 5, bottom panel), we can closely reproduce the cyclic voltammogram previously published.<sup>3b</sup> It is worth noting that a reversible CV peak at  $\sim 1.2$ – $1.3$  V can also be generated by multiple oxidation–reduction cycles on pure **1**. Thus, we suggest that prior literature results on the electrooxidation of **1** can be explained by either the presence of DBP as an impurity or the generation of DBP from electrooxidation of **1**.

## Discussion

The cation radicals of 1,2-diaryl-1,1,2,2-tetramethyldisilanes **1**–**3** were successfully generated in hexafluoroisopropanol (HFIP) at room temperature. **1**<sup>++</sup>–**3**<sup>++</sup> were found to rapidly react with both HOME and HOBu<sup>t</sup>. We attribute the  $\sim 4$ - to 5-fold lower reactivity of HOBu<sup>t</sup> to a steric effect.

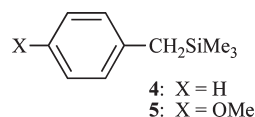
(17) (a) Ronlán, A.; Coleman, J.; Hammerich, O.; Parker, V. D. *J. Am. Chem. Soc.* **1974**, *96*, 845. (b) Park, S. M.; Bard, A. J. *J. Chem. Phys. Lett.* **1976**, *38*, 257.

(18) 4,4'-Dimethoxybiphenyl is a plausible byproduct of the 4-methoxyphenyl magnesium bromide used to prepare **1** in ref 3. Our samples of **1**–**3** were shown to contain  $< 0.03\%$  of the corresponding biphenyls (see the Experimental Section).

This reactivity difference is similar to that found for nucleophilic substitution at silicon on the similarly reactive cation radical of benzyltrimethylsilane. On the basis of this similarity and the known propensity for Si–Si bond fragmentation in disilane oxidations,<sup>1</sup> we ascribe the reactions of **1**<sup>++</sup>–**3**<sup>++</sup> with alcohols to nucleophile-assisted fragmentation of the Si–Si bond.

As noted above, the reactivities of **1**<sup>++</sup>–**3**<sup>++</sup> are remarkably similar. This contrasts with the  $> 65$ -fold difference in reactivity for the cation radicals of benzylsilanes **4** and **5** (see below) with HOME in HFIP.<sup>4</sup> The differences can now be readily explained by the relative oxidation potentials, which are a good predictor of relative cation radical reactivity.<sup>10</sup> For example, the oxidation potential of **4** is 0.5 V greater than **5**, which explains the much higher reactivity of **4**<sup>++</sup>. In contrast, the oxidation potentials of **1**–**3** differ by only  $\sim 0.02$  V, which explains the similar reactivities of their cation radicals.

Given the relatively large differences in both the oxidation potentials and relative reactivities of **4**<sup>++</sup>–**5**<sup>++</sup> vs **1**<sup>++</sup>–**3**<sup>++</sup>, it is interesting to note that the cation radicals exhibit dramatically opposite trends in their visible absorptions. The absorption spectra of **4**<sup>++</sup> (530 nm) and **5**<sup>++</sup> (500 nm) differ by only 30 nm, with the *p*-methoxy derivative absorbing at shorter wavelength.<sup>4</sup> In contrast, the *p*-methoxy-substituted disilane cation radical, **1**<sup>++</sup>, absorbs at *longer* wavelength than **3**<sup>++</sup>, and by  $\sim 240$  nm! A compelling rationalization of these markedly different results will require an assignment of the electronic transitions for the benzylsilane and disilane cation radicals.



The ability to determine the oxidation potentials of **1**–**3** by the redox equilibrium method is noteworthy, especially given the high reactivities of the disilane cation radicals. This provides yet another example of the power of the methodology.<sup>19</sup> Finally, we note that, due to the high reactivities of disilane cation radicals toward nucleophiles, the oxidations of disilanes **1**–**3** are not reversible by conventional cyclic voltammetry. Nor do we expect the electrochemical oxidations of similarly substituted disilanes to be reversible, although it may be possible to obtain reversible behavior with ultrafast potentiostats and microelectrodes.<sup>20</sup> Nevertheless, as described here, slow scan CV combined with rate data from laser flash photolysis (LFP) can provide redox potentials with accuracy and precision comparable to those established by the redox equilibrium method. The CV-LFP approach should find greater use in determining thermodynamically meaningful redox potentials for compounds that form highly reactive ion radicals upon oxidation or reduction.

(19) For application of this method to the determination of oxidation potentials for primary amines, see: Bourdelande, J. L.; Gallardo, I.; Guirado, G. *J. Am. Chem. Soc.* **2007**, *129*, 2817.

(20) (a) Wightman, R. M.; Wipf, D. O. *Electroanal. Chem.* **1989**, *15*, 267. (b) Andrieux, C. P.; Hapiot, P.; Savéant, J.-M. *Chem. Rev.* **1990**, *90*, 723. (c) Heinze, J. *Angew. Chem., Int. Ed. Engl.* **1993**, *32*, 1268. (d) Amatore, C.; Bouret, Y.; Maisonhaute, E.; Abruna, H. D.; Goldsmith, J. I. C. R. *Chim.* **2003**, *6*, 99. (e) Amatore, C.; Maisonhaute, E.; Simmoneau, G. *Electrochem. Commun.* **2000**, *2*, 81. (f) Amatore, C.; Maisonhaute, E.; Simmoneau, G. *J. Electroanal. Chem.* **2000**, *486*, 141.

## Experimental Section

**Materials.** Acetonitrile was purified by passing the solvent over a bed of activated alumina.<sup>21</sup> Hexafluoroisopropanol was successively distilled from sodium bicarbonate and activated molecular sieves (3 Å) under N<sub>2</sub>. Toluene was distilled under N<sub>2</sub>. Spectral-grade methanol and *tert*-butanol were obtained from commercial sources and used as received. 1,2,4,5-Tetramethoxybenzene was generously provided by Kodak. *N*-Methylquinolinium hexafluorophosphate was prepared by a literature method.<sup>4</sup> Hexaethylbenzene (Kodak) was purified by recrystallization from ethanol. Tetra-*n*-butylammonium tetrafluoroborate (Fluka, electrochem. grade) was used as received. Disilanes **1–3** were prepared by a literature method<sup>22</sup> and were purified by repeated recrystallization from ethanol/ethylacetate, methanol/ethyl acetate, and methanol, respectively. Gas chromatographic analysis (HP Ultra 2, 9.6 m × 0.2 mm × 0.33 μm) of **1–3** showed that the disilanes contained <0.03% of the corresponding biphenyls as impurities.

**Transient Absorption Experiments.** Detailed descriptions of the nanosecond and picosecond transient absorption apparatus are given elsewhere.<sup>12</sup> *N*-Methyl quinolinium hexafluorophosphate solutions (OD ≈ 0.5–1.0 at 343 nm) containing 1 M toluene were prepared in HFIP or acetonitrile. Experiments were conducted in quartz cuvettes equipped with high vacuum stopcocks that carried serum caps. Solvent-saturated dioxygen was bubbled through the solutions for 10–15 min before equilibrium measurements were made. For redox equilibration experiments, separate solutions were initially prepared with each of the components in order to record the spectra of their corresponding cation radicals. Then, increasing concentrations of the second component were added to one of the cuvettes from a dioxygen-saturated stock solution via a calibrated gas-tight syringe equipped with a 6 in. 22 gauge fixed needle. All equilibrium measurements were made at 20 °C. In general, equilibrium

measurements were made at least 100 ns after the laser pulse. At the end of each equilibrium experiment the spectrum of the sample containing the single equilibrium component was re-recorded to ensure that the laser power had not changed during the course of the experiment. Equilibrium spectra were fit as previously described.<sup>12a</sup> The oxidation potential differences given in Table 2 are an average of at least three independent determinations. In experiments where the influence of adventitious water was to be minimized, the solutions were dried by storage over 3 Å activated molecular sieves for > 2 h.

**Cyclic Voltammetry.** Oxidation potentials were measured with a BAS-100B/W Electrochemical Workstation or a computer-controlled VSP-potentiostat (Versatile Modular Potentiostat). Scan rates were in the range 0.1–50 V/s and positive feed-back *iR* compensation was used throughout. Experiments were conducted with a standard three-electrode setup in a conical electrochemical cell enclosed in a jacket that allowed the temperature to be maintained at 20 °C by means of a thermostated circulating bath. The working electrode was a glassy carbon disk (1.0 mm dia.) that was polished with a 1 μm diamond paste. The counter electrode was a glassy carbon disk (0.3 cm diameter). All of the potentials are reported vs an SCE electrode that was isolated from the working electrode compartment by a salt bridge with a ceramic frit that allowed ionic conduction between the two solutions while avoiding appreciable contamination. Solutions were prepared with HFIP or acetonitrile as a solvent and they were purged with argon before the measurements were made. The concentration of the electroactive substances was ~10<sup>-3</sup> M. The supporting electrolyte was 0.1 M tetra-*n*-butylammonium tetrafluoroborate.

**Acknowledgment.** Research was supported by a grant from the National Science Foundation (CHE-0749919). G.G. is grateful to the Spanish Ministerio de Ciencia e Innovación for financial support (CTQ2009-07469). We are grateful to Eastman Kodak for generously providing a sample of 1,2,4,5-tetramethoxybenzene.

(21) (a) Pangborn, A. B.; Giardello, M. A.; Grubbs, R. H.; Rosen, R. K.; Timmers, F. J. *Organometallics* **1996**, *15*, 1518. (b) Alaimo, P. J.; Peters, D. W.; Arnold, J.; Bergman, R. G. *J. Chem. Educ.* **2001**, *78*, 64.

(22) Kelling, H. Z. *Chem. (Stuttgart, Ger.)* **1967**, *7*, 237.